

## Self-Stratification During Film Formation from Latex Blends Driven by Differences in Collective Diffusivity

Irina Nikiforow, Jörg Adams, Alexander M. König, Arne Langhoff, Katja Pohl, Andrey Turshatov,<sup>†</sup> and Diethelm Johannsmann\*

*Institute of Physical Chemistry, Clausthal University of Technology, Arnold-Sommerfeld-Str. 4, D-38678 Clausthal-Zellerfeld, Germany. <sup>†</sup>Present address: MPI for Polymer Research, Ackermannweg 10, 55128 Mainz, Germany.*

*Received April 28, 2010. Revised Manuscript Received June 20, 2010*

Coatings with vertical gradients in composition were produced by drying an aqueous polymer dispersion containing both charged and neutral particles. After drying, the neutral component was enriched at the film/air interface. The spontaneous vertical segregation between the two types of particles goes back to a difference in collective diffusivity. As the film dries, a layer enriched in polymer develops at the top. Due to their mutual repulsion, charged spheres escape from this layer more quickly than their neutral counterparts. Provided that the total time of drying is between the times of diffusion for the two types of particles ( $\sim H_0^2/D_c$  with  $H_0$  the initial film thickness and  $D_c$  the collective diffusivity of the respective species), a concentration gradient persists after the film has turned dry. This effect can be used to create a functionally graded material (FGM) in a single coating step.

### Introduction

Technical paints are classical examples of multifunctional materials.<sup>1</sup> Typically, they protect the substrate mechanically, inhibit corrosion, and provide color and gloss. Not surprisingly, most coatings are structured vertically. For instance, automotive coatings are composed of at least three layers. There is an electrodeposition resin<sup>2</sup> at the bottom, optimized for adhesion and corrosion protection, a base coat, containing most of the pigments, and a top coat, optimized for gloss and scratch resistance.<sup>3</sup> Actually, more than three layers are frequently encountered. Even with a single function in mind, a vertically graded coating may have superior performance. Scratch resistance<sup>4</sup> is an example: a hard top minimizes adhesion of the indenting object, while a more compliant bottom dissipates mechanical energy, thereby reducing the danger of brittle fracture.

A straightforward way of producing vertically structured coatings is multistep deposition. This approach is flexible. Even different deposition techniques (such as electrodeposition and powder coating) may be employed in the different steps. However, it would certainly be attractive to produce such graded coating in a *single step*, as well. This would shorten production time and reduce cost.

Single-step generation of materials with spatial gradients in composition and function is well-known from the field of ceramics.<sup>5,6</sup> The resulting products carry the name “functionally graded materials (FGMs)”. Technically speaking, the term “functionally graded” should apply to just about every coating, as well. However, we use it to denote films exhibiting spontaneous vertical segregation

or “self-stratification”<sup>7–10</sup> in the sense discussed below. In ceramics, composition gradients are created by sedimentation. In a dispersion of *neutral* particles, larger particles sediment faster than average and are therefore *enriched* at the bottom. Interestingly, the reverse effect is observed for charged particles.<sup>11,12</sup> The phenomenon carries the name “colloidal brazil nut effect”.<sup>13</sup> The colloidal brazil nut effect and the segregation reported below are related phenomena.

In the coatings field, spontaneous layering is also known as “self-stratification”.<sup>7,14–18</sup> For films cast from solutions of polymer mixtures, surface-directed demixing may occur due to a preferential wettability of the substrate by one of the components.<sup>19</sup> Due to the short range of most surface forces, this concept is only applicable to rather thin films, typically around a few hundred nanometers, at most. As a second example, Ciba (now part of BASF) advertises a method to generate hard/soft gradients in a film based on a variable efficiency of photocross-linking.<sup>20</sup> The cross-linking agent is designed such that the film is most tightly cross-linked at the top, which leads to an improved scratch resistance.

We report on a novel mechanism leading to self-stratification, driven by the vertical flow of water during drying of a latex film.<sup>21–23</sup> Figure 1 illustrates the principle. In the initial stage of the film formation process, all components are mobile and the

\*To whom correspondence should be addressed. E-mail: johannsmann@pc.tu-clausthal.de.

(1) Wicks, Z. W.; Jones, F. N.; Pappas, S. P.; Wicks, D. A. *Organic Coatings: Science and Technology*; Wiley: New York, 2007.

(2) Dini, J. W. *Electrodeposition: The Materials Science of Coatings and Substrates*; Noyes Publications: Norwich, NY, 1993.

(3) Xiang, C.; Sue, H. J.; Chu, J.; Coleman, B. J. *Polym. Sci. Part B-Polym. Phys.* **2001**, *39*, 47.

(4) Dasari, A.; Yu, Z. Z.; Mai, Y. W. *Mater. Sci. Eng. R-Rep.* **2009**, *63*, 31.

(5) Okubo, T.; Okamoto, J.; Tsuchida, A. *Colloid Polym. Sci.* **2008**, *286*, 941.

(6) Biesheuvel, P. M.; Verweij, H. J. *Am. Ceram. Soc.* **2000**, *83*, 743.

(7) Carr, C.; Wallstom, E. *Prog. Org. Coat.* **1996**, *28*, 161.

(8) Rhudy, K. L.; Su, S.; Howell, H. R.; Urban, M. W. *Langmuir* **2008**, *24*, 1808.

(9) Verkholtantsev, V. V. *Pigment Resin Technol.* **2003**, *32*, 300.

(10) Urban, M. W. *Europ. Coat. J.* **2003**, *1–2*, 36.

(11) Zwanikken, J.; van Roij, R. *Europhys. Lett.* **2005**, *71*, 480.

(12) Cuetos, A.; Hynninen, A. P.; Zwanikken, J.; van Roij, R.; Dijkstra, M. *Phys. Rev. E* **2006**, *73*, 8.

(13) Masliyah, J. H.; Bhattacharjee, S. *Electrokinetic and Colloid Transport Phenomena*; Wiley: New York, 2006.

(14) Walbridge, D. J. *Prog. Org. Coat.* **1996**, *28*, 155.

(15) Kuczynska, H.; Langer, E.; Kaminska-Tarnawska, E.; Lukaszczuk, J. *Polimery* **2009**, *54*, 91.

(16) Budkowski, A.; Bernasik, A.; Moons, E.; Lekka, M.; Zemla, J.; Jaczewska, J.; Haberk, J.; Raczowska, J.; Rysz, J.; Awiuk, K. *Acta Phys. Polym.* **2009**, *115*, 435.

(17) Verkholtantsev, V. V. *J. Coat. Technol.* **1992**, *64*, 51.

(18) Schmidt, H.; Naumann, M.; Muller, T. S.; Akarsu, M. *Thin Solid Films* **2006**, *502*, 132–137.

(19) Jones, R. A. L.; Norton, L. J.; Kramer, E. J.; Bates, F. S.; Wiltzius, P. *Phys. Rev. Lett.* **1991**, *66*, 1326.

(20) <http://www.ciba.com/pic-ind-pc-tech-surface-scratch1.jpg>, downloaded on May 11, 2009.

(21) Keddie, J. L. *Mater. Sci. Eng. R-Rep.* **1997**, *21*, 101.

(22) Steward, P. A.; Hearn, J.; Wilkinson, M. C. *Adv. Colloid Interface Sci.* **2000**, *86*, 195.

(23) Winnik, M. A. *Curr. Opin. Colloid Interface Sci.* **1997**, *2*, 192.

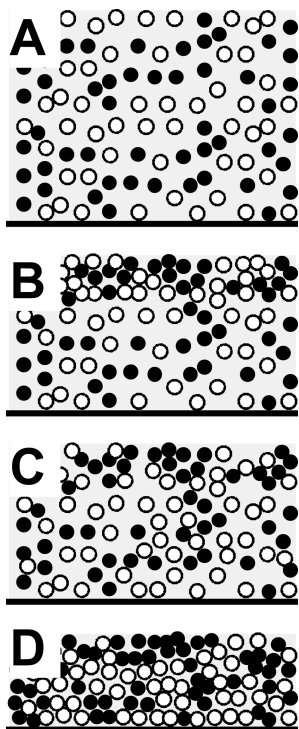


**Figure 1.** Cartoon of segregation based on collective diffusivity during drying. A: Particles are evenly distributed. B: A layer of enriched particles forms at the film/air interface due to evaporation of water. C: Due to electrostatic repulsion, charged particles (open dots) escape the skin faster than neutral particles (full dots). While charged particles equilibrate their concentration profile quickly, neutral ones do not. D: Provided that the drying time is such that charged particles stay close to diffusion equilibrium while neutral ones fall out of equilibrium, neutral particles are enriched at the top of the coating after drying is complete.

composition of the film is uniform (A). Evaporation depletes the water at the film/vapor interface and thereby enriches all other components relative to the bulk of the film (B).<sup>24,25</sup> If some species diffusively equilibrate this concentration gradient faster than others, a difference in concentration *between* the different species develops (C). Provided that the time of drying is chosen properly, this concentration gradient is eventually frozen in. In the dry film, the slow and the fast components are enriched at the top and the bottom, respectively (D). For reasons discussed in the Discussion section, spontaneous segregation (that is, enrichment of the neutral component and depletion of the charged one) mostly occurs at the film–air interface. Of course the remaining part of the film shows corresponding differences in concentration, but the effect is most impressive close to the upper surface.

Here, we report on spontaneous segregation driven by *charge*. Employing a latex blend of charged and neutral particles, we found that vertical segregation between the two species readily occurred. Below, we elaborate on the experimental conditions leading to segregation and show that self-stratification here is driven by collective diffusion – as opposed to preferential agglomeration or to specific interactions between the particles and the film/substrate interface.

### Materials

The experiments were carried out with acrylic latex blends prepared by miniemulsion polymerization.<sup>26,27</sup> Hexadecane was

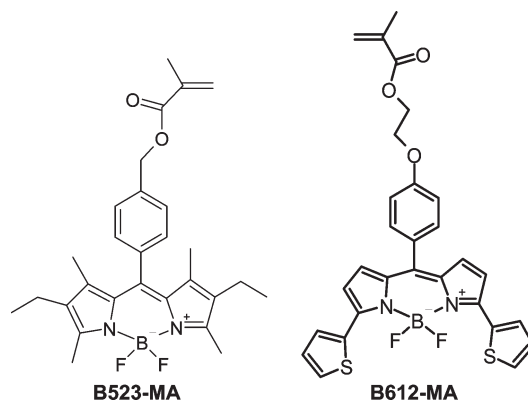


**Figure 2.** Chemical structure of the dyes, which are derivatives of boron-dipyrromethene (BODIPY).

added as the hydrophobe at a concentration of 4 wt %. The polymerization was started by the oil-soluble initiator  $\alpha, \alpha'$ -azobisisobutyronitrile (AIBN, 1.5 wt %). All concentrations are relative to the monomer base. We employed a nonionic surfactant, namely Lutensol AT50 (BASF). Lutensol AT50 contains 50 units of polyethylene oxide as its hydrophilic part. These rather long hydrophilic chains provide for steric stabilization. Note that the emulsifier is neutral. Similar experiments with an ionic emulsifier (such as sodium dodecyl sulfate, SDS) would have been problematic because a charged surfactant might exchange between particles, thereby equilibrating the charge between the two species. The organic phase (monomers, hydrophobe, dyes, and initiator) and the aqueous phase (water, surfactant) were mixed in a ratio of 1:4 and stirred under ice cooling for 5 min. The miniemulsion was prepared by ultrasonication at an amplitude of 70% (Branson sonifier W450 Digital, 1/2 in.-tip). Polymerization occurred overnight at 70 °C. The solids content after polymerization was 23 wt %. The particle diameters as determined by dynamic light scattering (DLS) were 120 and 119 nm for the charged and the neutral fraction, respectively. The amount of surfactant added to the recipes had been adjusted in order to ensure equal particles sizes for the neutral and the charged fraction, thereby excluding a size difference as the driving force behind segregation.

The monomer base of the neutral particles consisted of methylmethacrylate (MMA) and butylacrylate (BA) in a ratio of 60:40 wt %. The ratio of 60:40 was chosen to obtain hard particles, which still form clear films at ambient conditions. For the charged particles, acrylic acid (AA) was added to the recipe at a level of 1.5 wt %. Acrylic acid is known to be enriched on the outside of the particles.<sup>28</sup> At a pH larger than the  $pK_a$  of acrylic acid (around 3 to 4), the latter type of particles is charged. The pH of the latex blend was adjusted to around neutral by addition of NaOH. The zeta potential as determined with a Zetasizer 3000 HSA (Malvern) was  $-37$  mV for the charged particles and  $-11$  mV for the nominally neutral particles. Technically speaking, the “neutral” particles should be called “nominally neutral” because they do carry some charge. We stick to the term neutral for brevity. In water, particles are almost never perfectly neutral for a number of reasons (adsorption of ions being among them). Before the experiment, equal amounts of charged and neutral particles were mixed, that is, a 1/1 latex blend of charged and neutral particles was employed.

The first sets of experiments (shown in Figure 4) were undertaken with labels on one species only (either charged or neutral). In these cases the dye B523-MA (left in Figure 2) was employed. Only one species is visible for every sample and the comparison has to be made under the assumption that the preparation conditions were the same. At a later stage, we employed two-color confocal microscopy (Figure 5), labeling both the charged and the uncharged fraction employing compound B523-MA and compound B612-MA. All labeling occurred at a level of 0.1%.

(24) Routh, A. F.; Russel, W. B. *Langmuir* **1999**, *15*, 7762.

(25) Routh, A. F.; Zimmerman, W. B. *Chem. Eng. Sci.* **2004**, *59*, 2961.

(26) Asua, J. M. *Prog. Polym. Sci.* **2002**, *27*, 1283.

(27) Antonietti, M.; Landfester, K. *Prog. Polym. Sci.* **2002**, *27*, 689.

(28) Reynhout, X. E. E.; Hoekstra, L.; Meuldijk, J.; Drinkenburg, A. A. H. *J. Polym. Sci., Part A* **2003**, *41*, 2985.

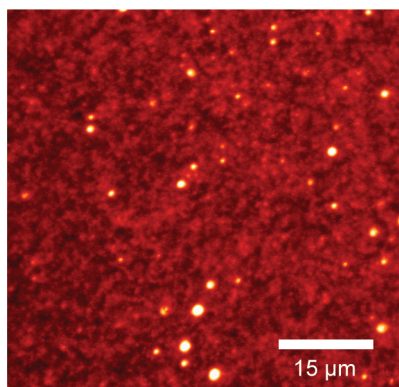


**Figure 3.** Typical raw image. The particle concentration was determined based on confocal laser scanning microscopy and particle counting.

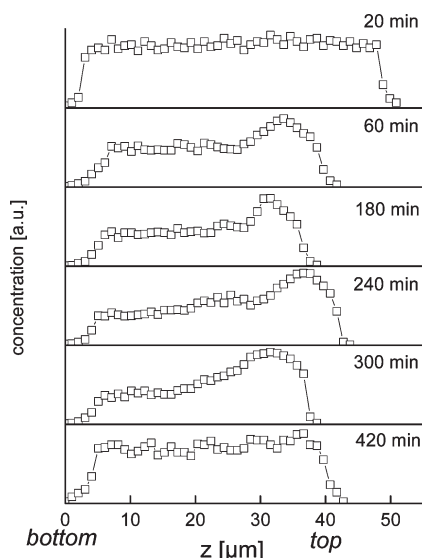


**Figure 4.** Concentration of neutral particles per frame vs depth,  $z$ , for a number of different drying rates. For very fast drying (top) and very slow drying (bottom) the collective diffusion is inefficient in creating segregation. One can only expect self-stratification if the drying time is in-between the two characteristic times of diffusion.

Only 1 out of 1000 particles is visible and the fluorescent particles were well separated from each other.

The dyes employed were polymerizable derivatives of boron-dipyrromethene (BODIPY), shown in Figure 2. The maxima of absorption and emission are at 523 and 536 nm, for B523-MA (left in Figure 2), and at 612 and 630 nm, for BA612-MA. The dye molecules were covalently attached to the polymer backbones, where the degree of labeling was 0.5%. Generally speaking, neither chemical stability nor stability against photobleaching are essential for the experiments reported below because the analysis relies on particle counting, rather than absolute measurements of brightness. Since the dye is neutral, it is not expected that the presence of the dye strongly affects the diffusivity of the particles.

### Acquisition of Profiles

An amount of 14  $\mu\text{L}$  of the dispersion was spread onto a microscope glass slide, spread out to an area of 100  $\text{mm}^2$  using a knife edge, and allowed to dry. The drying rate was controlled by enclosing the sample in a compartment with a small hole. Opening the hole resulted in a drying time of 20 min. By gradually closing the hole, the drying time could be varied. “Drying time” here is defined as the time until the center of the sample turns transparent.

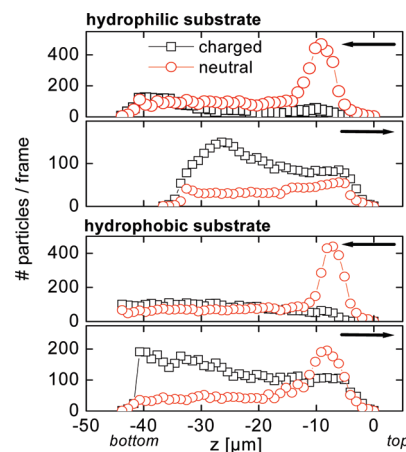


**Figure 5.** Number of particles per frame for a typical experiment. These data were acquired with two-color confocal microscopy on a hydrophilic and a hydrophobic substrate. Arrows indicate the direction of incident light.

The determination of particle concentration occurred by means of confocal scanning microscopy, using the SP2 instrument from Leica. Figure 3 shows typical raw data. Only neutral particles were labeled in this case. The number of bright particles per frame was counted, using the software package Q-Win (Leica). While the raw data suggest that a few aggregates may be present (cf. Figure 3), no attempt was made to correct for the related artifacts. Each frame corresponds to a slice of  $\Delta z = 1 \mu\text{m}$  in thickness.

For all samples images were taken from both the top (the film/air interface) and the bottom (the film/substrate interface). There were slight systematic differences between these data sets, because particles at the rear end of the imaging volume have a lower detection probability. We show profiles taken from the top as well as from the bottom in Figure 5. Arrows indicate the direction of the incident light. Note that these profiles were not acquired at the exact same spots.

## Results

Figure 4 shows the number of particles per sheet versus distance from the substrate for different drying times. Apart from the evidence for segregation, per se, two other features are noteworthy. First, the accumulation of neutral particles mostly happens immediately below the film/air interface. The profile is flat for large parts of the bulk film. Second, segregation does *not* occur, if the drying time is either very short or very long. We will come back to these observations in the Discussion section.

Figure 5 shows a data set acquired with dual labeling (that is, labeling of the charged and the neutral fraction with different colors). The interpretation needs to be done with care because there is some cross-sensitivity between the two channels. Still, one can clearly see that the concentrations of charged and neutral particles are anticorrelated. The figure also points to some further problems. First, the sum of the two profiles is not constant. Although one always hopes that the fluorescently labeled particles faithfully represent the distribution of the larger ensemble (neutral or charged, nonlabeled), there clearly is some influence of labeling on particle position. Such an influence does not invalidate the argument, as such. Segregation *is* observed but the immediate evidence only covers the fluorescent particles. Even some influence of labeling acknowledged, there must be a physical reason for segregation. Second, a caveat derived from Figure 5 concerns the differences between samples observed from the air side and the substrate side. The arrows in Figure 5 denote the



direction of the incident light. Since the substrates were only 30  $\mu\text{m}$  thick, one can image the sample through the substrate and compare to the profiles acquired from the top. As the figure shows, all concentration gradients are more pronounced on the side facing the microscope. Particle counting has not completely eliminated artifacts of variable visibility of the particles. Concerning the proof of segregation, these technical shortcomings are irrelevant.

We focus on vertical segregation, but lateral segregation certainly is expected for the same reasons. Typically a drying front propagates from the edge toward the center of a film and there is a rich scenario of processes at the drying front.<sup>29</sup> In particular, the charged particles should be able to escape the drying front more efficiently than the neutral ones, which induces segregation. Presumably, one will attempt to limit lateral segregation in practice, but, again, lateral and vertical segregation are connected.

## Discussion

Before elaborating collective diffusion, which we claim to be the source of self-stratification, we discuss two other potential mechanisms, which we discard. We call them “preferential wetting” and “preferential aggregation”. There is a rich literature on how the wettability of the substrate by one component of a binary polymer blend induces layering.<sup>30</sup> In order to check for this mechanism, we have performed drying experiments on a glass substrate and on a polystyrene substrate, where the former is hydrophilic and the latter is hydrophobic. As Figure 5 shows, the results are similar, which rules out “preferential wetting” as the driving force. These experiments only covered the substrate. There is a possibility of preferential wetting of the neutral species at the film/air interfaces as well. Equivalently, one might argue that acrylic acid is repelled from the film/air interface. While our experiments do not strictly rule out this possibility, the fact that preferential wetting did not take place at the film/substrate interface speaks against preferential wetting at the film/air interface.

“Preferential aggregation” implies a mechanism by which the neutral particles coalesce more easily than the charged ones, thereby forming a neutral skin.<sup>31–33</sup> In order to check for this possibility, we investigated both the charged and the neutral dispersion by ultracentrifugation. Both samples did sediment, but both samples spontaneously redispersed after the centrifuge had been turned off, even though sedimentation had produced what looked like a “cake” in the bottom part of the cell. Under these conditions, neither the neutral nor the charged fraction had aggregated. This makes sense in view of the fact that a long-chain nonionic emulsifier was employed, which provides for good stability. We therefore rule out preferential aggregation as the driving mechanism, as well.

In the following, we elaborate on why, in general, variable diffusivity may lead to segregation. There are two reasons, why some particles might diffuse slower than others. First, there may be segregation by size. Diffusivity scales inversely with particle size and one may expect the large particles to eventually reside at the top. The diffusivity between particles may vary by up to factor

of 10 if the size distribution is correspondingly large. A second and equally important source of variable diffusivity is charge.<sup>34,35</sup> Charged particles strongly resist enrichment at the film/air interface because of their mutual repulsion. They are driven away from the surface by electrostatic forces. Neutral particles also experience repulsion, but this repulsion is short-ranged. When the hard-core potential starts to be felt, close packing is almost reached. At this time, the dense packing prevents rearrangements of the particles and the concentration profiles of the two species relative to each other are fixed.

Central to the argument is the notion of cooperative diffusion, that is, diffusion under the influence of interactions between the particles. Central to the argument is the notion of cooperative diffusion, that is, diffusion under the influence of interactions (see appendix B). The cooperative diffusivity differs from the Stokes-Einstein diffusivity because of, firstly, hydrodynamic interactions, and, secondly, a nontrivial dependence of the chemical potential.  $D_c$  accounts for interactions, while  $D_0$  does not. Interactions come into play in two different forms. First, hydrodynamic interactions slow down diffusion ( $K(c) < 1$ ). Second, mutual repulsion increases the osmotic pressure and thereby speeds up transport.

Segregation by size does not rely on concentration. The second effect drives segregation by charge. The detailed calculation shows that diffusion driven by charge can be orders of magnitude faster than diffusion driven by entropy only (that is, by Stokes–Einstein diffusion).<sup>29</sup> A finite element calculation demonstrating segregation by collective diffusion is provided in Appendix B. It turns out, that there is a second critical parameter apart from the difference in diffusivities between the species. Segregation only occurs if the hydrodynamic coupling *between* the species is weak, initially, and becomes stronger, later on. If the motion of the particles is locked together at all times, the charged particles drag the neutral ones along. However, the relative motion must be frozen in at some later time in order to prevent reequilibration. Hydrodynamic coupling is indeed expected to be weak for dilute dispersions (initial phase of drying) and to increase later on. For this reason, segregation only occurs in the initial phase of the drying process. We believe this to be reason for the asymmetric profiles (Figure 4). Segregation starts from the film/air interface and it only happens in the initial phase of drying. Therefore the concentration gradients even after complete drying are most pronounced at the top.

Within this kinetic argument, one can understand why segregation does not occur if the drying is either very fast or very slow (Figure 4). For fast drying, the initial period, where the two species move at different speed, does not suffice to achieve appreciable segregation. The particle motion is locked, before segregation has come into effect. For very slow drying, segregation does happen, but the hydrodynamic coupling occurs too late to freeze it in. The asymmetric profiles equilibrate before drying is complete.

This mechanism of self-stratification should be easy to implement on a wide range of coating recipes. It relies on the correct choice of the initial solids content and the drying time. The solids content must be low enough to allow for significant movement of the particles relative to each other. At the same time, the drying must not be too long, in which case *all* particles would diffusively equilibrate their concentration gradients.

(29) Salamanca, J. M.; Ciampi, E.; Faux, D. A.; Glover, P. M.; McDonald, P. J.; Routh, A. F.; Peters, A.; Satguru, R.; Keddie, J. L. *Langmuir* **2001**, *17*, 3202–3207.

(30) Budkowski, A. *Advances in Polymer Science* **1999**, *148*, 1–111.

(31) Narita, T.; Beauvais, C.; Hebraud, P.; Lequeux, F. *Eur. Phys. J. E* **2004**, *14*, 287.

(32) Erkselius, S.; Wadso, L.; Karlsson, O. J. *J. Colloid Interface Sci.* **2008**, *317*, 83.

(33) Koenig, A. M.; Weerakkody, T. G.; Keddie, J. L.; Johannsmann, D. *Langmuir* **2008**, *24*, 7580.

(34) Bowen, W. R.; Mongruel, A. *Colloids Surf., A* **1998**, *138*, 161.

(35) Branca, C.; Faraone, A.; Lokotosh, T.; Magazu, S.; Maisano, G.; Malomuzh, N. P.; Migliardo, P.; Villari, V. J. *Mol. Liquids* **2001**, *93*, 139.

## Conclusions

Drying latex blends containing charged and neutral particles, one finds vertical gradients in composition. The neutral particles are enriched at the film/air interface. This type of self-stratification requires that the time of drying is in-between the characteristic times of diffusion of the charged and the neutral particles. The driving force behind the segregation is the repulsion between charged particles. Shortly after spreading, both the charged and the neutral particles are enriched at the film/vapor interface because of evaporation. However, charged particles equilibrate this concentration gradient faster than neutral ones, thereby creating a difference in concentration. If the drying time is chosen correctly, this concentration gradient persists after drying.

**Acknowledgment.** The authors acknowledge stimulation discussions with Joe Keddie. Alex Routh has proposed a similar mechanism based on size (rather than charge) and shared numerous valuable insights. The zeta-potential measurements were performed by Gabriele Vidrich from the Institut für Werkstoffkunde und Werkstofftechnik from Clausthal University of Technology. This work was partly funded by the EU under contract IP 011844-2 (NAPOLEON).

## Appendix A: Synthesis of Component B612-MA

In the synthesis of compound B523-MA, we followed ref 36. Below, we provide some details on the preparation of compound B612-MA. Figure 6 shows essential intermediates. Intermediate 1 was synthesized by the Mitsunobu reaction under conditions described in ref 37 with yield of 71%. Compound 2 was prepared with a yield of 60%. Finally, coupling 1 and 2 produced the compound B612-MA in form of red crystals (yield 41%).

All solvents (Sigma Aldrich, Fisher Sci.) were spectroscopic grade and were used without further purification. *N*-(*t*-Butoxycarbonyl)-pyrrole-2-boronic acid was purchased from Frontier Scientific. All other chemicals were purchased Sigma-Aldrich and used as received.

NMR spectroscopy of compound B612-MA:  $^1\text{H}$  NMR (300 MHz,  $\text{CDCl}_3$ )  $\delta$  8.21 (dd,  $J=1.0, 3.9$ , 2H), 7.50 (t,  $J=1.9$ , 2H), 7.47 (dd,  $J=1.9, 4.4$ , 2H), 7.24–7.16 (m, 2H), 7.10–7.00 (m, 2H), 6.87–6.77 (m, 4H), 6.18 (s, 1H), 5.62 (m, 1H), 4.62–4.52 (m, 2H), 4.32 (dd,  $J=3.4, 6.2$ , 2H), 1.97 (s, 3H).  $^{13}\text{C}$  NMR (75 MHz,  $\text{CDCl}_3$ )  $\delta$  167.29, 160.21, 149.94, 140.96, 136.70, 135.97, 134.33, 132.16, 131.30–130.90, 129.98, 129.01, 127.28, 126.18, 120.50, 114.50, 66.14, 62.91, 18.31. MS (FD),  $m/z$ : 559 ( $\text{M}^+$ ), calculated 560.

Figure 7 shows the absorption as well as the emission spectrum of the compound B612-MA.

## Appendix B: Modeling with Finite Element Analysis

In order to substantiate the arguments from the Discussion section, we have solved the corresponding set of partial differential equations employing finite element analysis (FEA). We used the Multiphysics software package from COMSOL, Göttingen, Germany.

At the core of the mechanism is collective diffusion, that is, diffusion under the influence of interactions between the particles. One has

$$D_c = D_0 K(c) c \frac{1}{RT} \frac{d\mu(c)}{dc} \quad (1)$$

(36) Garcia-Moreno, I.; Costela, A.; Campo, L.; Sastre, R.; Amat-Guerri, F.; Liras, M.; Lopez Arbeloa, F.; Banuelos Pietro, J.; Lopez Arbeloa, I. *J. Phys. Chem. A* **2004**, *108*, 3315.

(37) Tei, T.; Sato, Y.; Hagiya, K.; Tai, A.; Okuyama, T.; Sugimura, T. *J. Org. Chem.* **2002**, *67*, 6593.

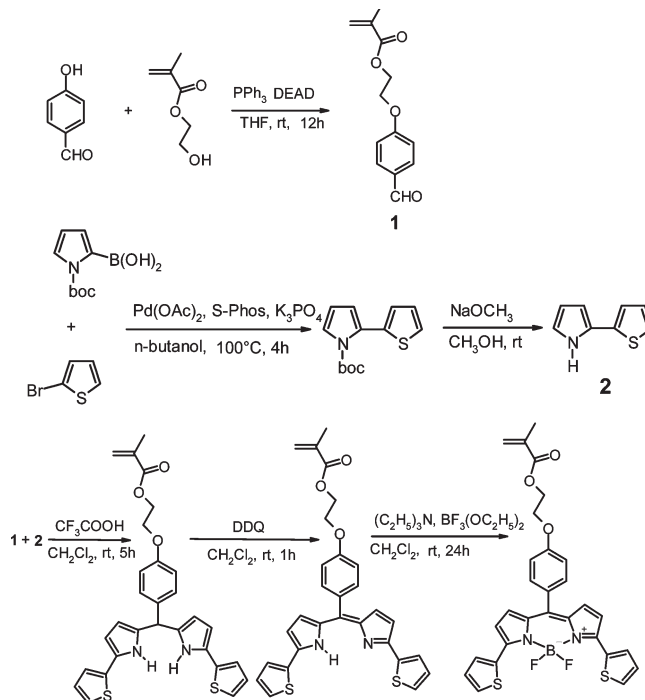


Figure 6. Steps of synthesis for compound B612-MA.

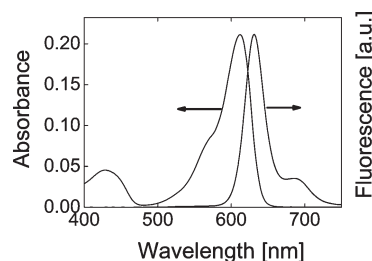


Figure 7. Absorption and emission spectra of compound B612-MA.

$D_c$  is the collective (also “cooperative”) diffusivity,  $D_0$  is the Stokes–Einstein diffusivity,  $c$  is concentration,  $K(c) < 1$  is the sedimentation coefficient (accounting for hydrodynamic interactions), and  $\mu(c)$  is the chemical potential.  $D_c$  accounts for interactions, whereas  $D_0$  does not. Interactions come into play in two different forms. First, hydrodynamic interaction slows down diffusion ( $K(c) < 1$ ). Second, mutual repulsion increases the osmotic pressure and thereby speeds up transport. In the following, we do not explicitly base the discussion on the chemical potential and sedimentation coefficient. We just assume some functions for the dependence of the collective diffusivities on concentrations, which make sense and lead to segregation. It should be possible to construct a more realistic model, explicitly inserting known relations for  $K(c)$  and  $\mu(c)$ . However, such a model would require either a very precise knowledge of the system under investigation, or further guesses in the input parameters.

Fick’s law for coupled diffusion is

$$\begin{aligned} J_1 &= D_{11} \nabla c_1 + D_{12} \nabla c_2 \\ J_2 &= D_{12} \nabla c_1 + D_{22} \nabla c_2 \end{aligned} \quad (2)$$

Indices denote the species (1: charged, 2: neutral).  $D$  is the (collective) diffusivity. Water is not part of the equation because the fluxes  $J_1$  and  $J_2$  determine the flow of water by volume conservation.

Importantly, a gradient in the concentration of one species may induce a flux of the second. The cross-coefficient,  $D_{12}$ , may be (and often is) nonzero. A nonzero  $D_{12}$  is, for instance, found when the two species are coupled hydrodynamically. Consider a blend of charged and neutral particles. Upon application of an electric field, a charged particle migrates along the field, while the neutral particle does not feel the electric field. However, the neutral particle still is expected to move in the field direction because it feels the drag exerted by its charged neighbors.

In a drying coating,  $D_{12}$  is expected to be small, initially. At some later time, the space needed for particle rearrangement decreases and the two movements are progressively locked together. For this reason, segregation only occurs during the initial phase and is confined to the region near the film/air interface.

We write the diffusivities as

$$D = (1 - \alpha(c_{\text{tot}}))D_{\text{dil}} + \alpha(c_{\text{tot}})D_{\text{conc}} \quad (3)$$

where  $\alpha(c_{\text{tot}})$  is a parameter between 0 and 1 and  $c_{\text{tot}} = c_1 + c_2$ .  $c_1$  and  $c_2$  are normalized such they numerically are the same as the volume fraction.  $D_{\text{dil}}$  is a set of diffusivities expected for dilute dispersions and  $D_{\text{conc}}$  is a second set expected in the limit of high concentration. For the parameter  $\alpha$ , we write

$$\alpha = \tanh\left(\frac{c_{\text{tot}}}{c_{\text{CO}}}\right) \quad (4)$$

$c_{\text{CO}}$  is the crossover concentration, which was chosen to correspond to a volume fraction of 0.3. The crossover concentration is an essential input to the model. For concentrations less than  $c_{\text{CO}}$ , the two species move independently. Above  $c_{\text{CO}}$ , the two species can only move relative to the liquid, they cannot move relative to each other.

The collective diffusivities in the dilute limit are given by

$$D_{\text{dil}} = \beta K(c)D_0 \quad (5)$$

$K(c)$  (the “sedimentation coefficient”) is a number  $<1$  accounting for hydrodynamic interactions,  $D_0$  is the Stokes–Einstein diffusivity, and  $\beta$  is a number accounting for the influence of the chemical potential.  $\beta$  was chosen as 1 for the neutral species and as 10 for the charged species. The sedimentation coefficient was chosen as  $K(c) = (1 - c_{\text{tot}})^{6.55}$ .<sup>38</sup> The coupling term was chosen as  $D_{12,\text{dil}} = 0$ .

In the limit of high concentration, the speeds of flow must be the same for the two species, which implies

$$\frac{J_1}{c_1} = \frac{D_{11}\nabla c_1 + D_{12}\nabla c_2}{c_1} = \frac{J_2}{c_2} = \frac{D_{12}\nabla c_1 + D_{22}\nabla c_2}{c_2} \quad (6)$$

Since this equality must hold for all concentration gradients, one has

$$\begin{aligned} \frac{D_{11,\text{conc}}}{c_1} &= \frac{D_{12,\text{conc}}}{c_2} \\ \frac{D_{12,\text{conc}}}{c_1} &= \frac{D_{22,\text{conc}}}{c_2} \end{aligned} \quad (7)$$

(38) Russel, W. B., Saville, D. A., Schowalter, W. R. *Colloidal Dispersions*; Cambridge University Press: New York, 1995.

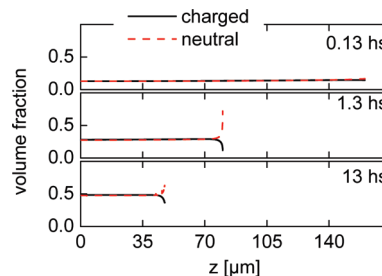


**Figure 8.** Concentration profiles for three different drying times as predicted by the simulation in Appendix B. Initially, the solids content is 25% with equal concentrations of charged and neutral fractions. After 13 h, the film is almost perfectly dry and the concentration gradient, which developed early in the process, is frozen in. After 13 h, the solids content is almost unity.

$D_{12,\text{conc}}$  was chosen as the geometric mean of  $D_{11,\text{dil}}$  and  $D_{22,\text{dil}}$ .

The drying rate,  $dH/dt$  ( $H$  the film thickness) was chosen as  $E_0(1 - c_{\text{tot}}(z = H))$ .  $E_0 = 3$  mm/day is the evaporation rate of pure water and the term in brackets is the water volume fraction at the film/air interface. The initial concentrations were  $c_{1,\text{ini}} = c_{2,\text{ini}} = 0.125$ . The initial film thickness was  $H_0 = 160$   $\mu\text{m}$ .

The solution, in principle, follows from numerical integration. There is further technical detail. In order to avoid a moving domain boundary, the model uses the scaled coordinate

$$\bar{z} = \frac{z}{H(t)} \quad (8)$$

In the following, a bar denotes the parameter which is scaled to film thickness. The moving coordinates have the following consequences:

- All derivatives must be scaled to film thickness:

$$\frac{d}{dz} \rightarrow \frac{1}{H} \frac{d}{d\bar{z}}$$

- All speeds and flows must be scaled to film thickness  $J \rightarrow H\bar{J}$
- An additional flow must introduced, compensating for the moving coordinates

$$J \rightarrow H\bar{J} + c \frac{z}{H} \dot{H} = H\bar{J} + c \frac{\bar{z}}{H_0} \dot{H}$$

- A source term must be inserted into Fick’s second law in order to account for the shrinking volume:

$$\dot{c} = -\nabla \bar{J} + c \frac{\dot{H}}{H}$$

With these transformations, COMSOL readily produces the concentration profiles versus time. Figure 8 shows some results. In particular, the model reproduces the experimental finding that segregation mostly occurs at the film/air interface.

The model is not quantitative because the diffusivities as a function of concentration were guessed. The model was designed to capture the essential requirements needed for self-stratification. Again, these are

- Diffusivities differing between the two species in the dilute limit.
- Initial concentrations below the crossover concentration (cf. eq 3).
- A drying time in-between the characteristic times of diffusion for the fast and the slow component.